



Trade Science Inc.

ISSN : 0974 - 7478

Volume 7 Issue 3

# Macromolecules

*An Indian Journal*

*Full Paper*

MMALJ, 7(3), 2011 [93-101]

## Polymer inclusion membrane: Effect of the chemical nature of the polymer and plasticizer on the metallic ions transference

Zioui Djamilia<sup>1</sup>, Arous Omar<sup>1,2\*</sup>, Amara Mourad<sup>1,2</sup>, Kerdjoudj Hacène<sup>1</sup>

<sup>1</sup>Laboratory of Hydrometallurgy and Inorganic Molecular Chemistry, USTHB Faculty of Chemistry, BP32 ElAlia, 16111, (ALGERIA)

<sup>2</sup>Center of Research in Physical and Chemical Analysis CRAPC, BP248 Algiers RP 16004, Algiers, (ALGERIA)

E-mail: mo\_amara@yahoo.fr

Received: 16<sup>th</sup> May, 2011 ; Accepted: 16<sup>th</sup> June, 2011

### ABSTRACT

The polymer inclusion membranes used for the selective transport and separation of metal species has emerged in recent years. In this work, a development of a novel class of membrane for performing copper and zinc ions separation is reported. The membrane is polymerized from cellulose triacetate (CTA) and other polymers (P4VP or PMMA) with crown-ethers incorporated into the polymer as a metal ion carrier using tris ethyl hexyl phosphate or dioctylphtalate as plasticizers. Structural modifications promoted by the nature of the plasticizer and polymer that affect metal ion migration in polymer inclusion membranes (PIMs) were evaluated using FTIR, Scanning Electron Microscopy (SEM), X-Ray Diffraction (DRX) and Thermogravimetric Analysis (TGA). An analysis of the effects of different polymers on copper (II) and zinc (II) transport using crown-ethers as carrier revealed differences in transport profiles that can be explained on the basis of the nature of polymer and plasticizer used. The transport flux and its efficiency depend on the chemical nature of the plasticizer. It can be perceived that TEHP ( $\eta = 10.2$  mPa.s,  $\epsilon_r = 4.8$ ) and DOP ( $\eta = 76$  mPa.s,  $\epsilon_r < 10$ ) produce the highest PIM transport of ions. The polarity and viscosity appear to be the main characteristics of the membrane plasticizer which affect the PIM transport. Indeed, the plasticizer polarity influences the chemical potential of metal ion partitioning into the membrane, whereas increasing the viscosity of the plasticizer decreases the rate of transport, most likely by inhibiting the diffusion process. © 2011 Trade Science Inc. - INDIA

### KEYWORDS

Polymer inclusion membranes;  
PIMs;  
Membrane extraction.

### INTRODUCTION

Liquid membrane processes have become an attractive alternative to conventional solvent extraction for selective separation and concentration of compounds such

as metals and acids from dilute aqueous solution because it combines in a single stage, an extraction and a stripping operation. In order to reduce the amounts of reactants and energy needed for separations and to decrease the environmental and economic impact of solvent extrac-

## Full Paper

tion separations, several membrane-based separation techniques have been proposed in the past 30 years<sup>[1-5]</sup>.

Among these, supported liquid membranes (SLM) have been extensively studied since they offer high transport rates and good selectivity, therefore being a very interesting option to overcome the solvent extraction downsides<sup>[6]</sup> (from a recent review on supported liquid membrane-based separations). Nevertheless, SLM show an inherent lack of stability that hinders their use in practical applications. Carrier mediated transport of metal ions across liquid membranes is one of the promising options for the recovery of metal values from various waste streams<sup>[7-16]</sup>.

This is of great relevance in the nuclear industry in view of the stringent nuclear waste management regulations. In this context, few attempts have been made for the recovery of radiologically toxic long-lived actinides and fission products viz. <sup>241</sup>Am, <sup>90</sup>Sr, <sup>137</sup>Cs employing extractants like octyl(phenyl) - N, N - diisobutyl carbamoyl methyl phosphine oxide (CMPO), dimethyl dibutyl tetradecyl - 1, 3 - malonamide (DMDBTDM) and crown ethers using membrane based techniques<sup>[17-19]</sup>. Polymer Inclusion Membrane (PIM) systems have been successfully designed for metal extraction using solvating-type extractants such as crown ethers, trioctylphosphine oxide (TOPO), tributyl phosphate (TBP) and  $\beta$ -diketones<sup>[20-25]</sup>. Several other kinds of carriers (alkyldithiophosphoric acids, alkylammonium salts and natural ionophores) have also been employed for this purpose<sup>[26,27]</sup>.

Alternatively, several authors have reported that polymer inclusion membranes (PIM) show good long-term stabilities, although in general lower fluxes can be obtained with this kind of membranes due to their high viscosity. Recently, a comparison between SLM and PIM performance has been reported by Paugam and Buffle<sup>[28]</sup>, who show that similar phenomena control Cu(II) facilitated transport across both types of membranes using lauric acid as carrier. However, they do not discuss on the stability of both membrane systems. In a similar way, Schow et al.<sup>[29]</sup>, compare the fluxes of K<sup>+</sup> through a cellulose tri-acetate (CTA)-2-nitrophenyloctyl ether (NPOE) PIM containing crown ether as carrier (DC18C6) with several other DC18C6-chloroform liquid membranes. These authors found that PIM fluxes were three orders of magnitude larger than those exhibited by the thin sheet and hollow fiber SLM.

In this work, we have synthesized a novel class of plasticized cellulose triacetate membranes modified by carrier incorporation that are selectively permeable to copper and zinc cations. The membranes polymer + plasticizer + carrier were characterized using chemical techniques as well as Fourier Transform Infra - Red (FTIR), Scanning Electron Microscopy (SEM), X-Ray Diffraction (DRX) and Thermo-gravimetric Analysis (TGA). A comparative study of transport mechanism across plasticized membranes called polymer inclusion membranes (PIM) has been made.

## EXPERIMENTAL PART

### Chemicals

Copper(II) nitrate, zinc(II) nitrate, chloroform, cellulose triacetate (CTA), poly4-vinyl pyridine (P4VP), polymethyl methacrylate (PMMA) and Tris (Ethylhexyl) Phosphate (TEHP) were analytical grade reagents obtained from Fluka company. Dioctyl phthalate (DOP) was product of Carlo Erba Company. The carrier: 12 crown 4 noted 12C4, 15 crown 5 noted 15C5 and dicyclohexane 24 crown 8 noted D24C8 were product of Aldrich Company. All reagents were used as received without further purification. The aqueous phases were prepared by dissolving the different reagents in distilled water.

Figure 1 represents the different polymers used in this work.

We used two plasticizers; Tris (Ethylhexyl) Phosphate noted (TEHP) and Dioctyl phthalate noted (DOP) (figure 2).

We used three crown-ethers as carrier (figure 3):

- 12-couronne-4 noted (12C4).
- 15-couronne-5 noted (15C5).
- Dicyclohexane-24 couronne-8 noted (D24C8).

### Membranes preparation

Polymer inclusion membranes were prepared according to the procedure reported by Sugiura et al.<sup>[30]</sup>. 0.1 g of cellulose triacetate (CTA) and 0.1g of poly-4-vinyl pyridine (P4VP) or poly methyl methacrylate (PMMA) were dissolved in 20 mL of chloroform and stirred for 4 hours. Then, 0.2 mL of tris-(2-ethylhexyl) phosphate (TEHP) or dioctyl phthalate (DOP) and 0.2 mL of carrier (crown-ether) were added under vigor-

ous stirring during 2 hours. The solution was transferred in a circular glass container and the solvent was allowed to evaporate slowly during 24 hrs to obtain a polymer

film with a smooth looking surface. The resulting membrane was extracted by addition of bi distilled water and dried at 40 °C.

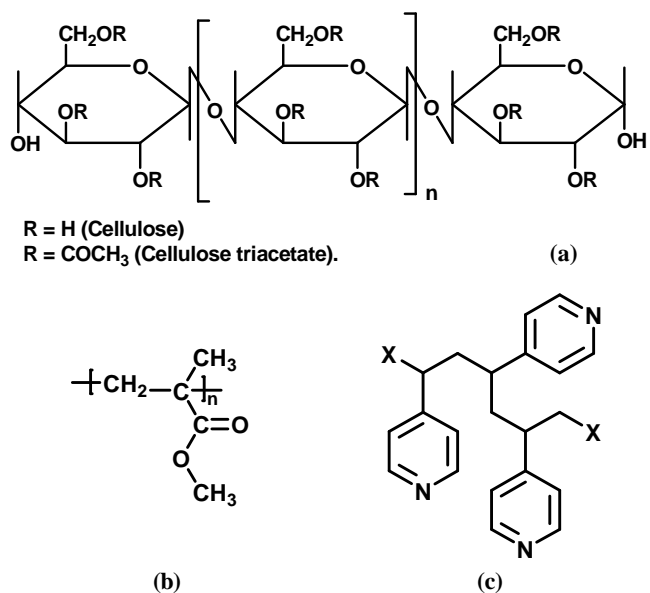


Figure 1 : Chemical Structures of polymers: (a) CTA; (b) PMMA; (c) P4VP

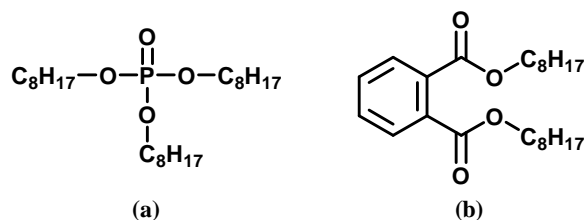


Figure 2 : Chemical structures of plasticizers used in the PIMs: (a) TEHP, (b) DOP.

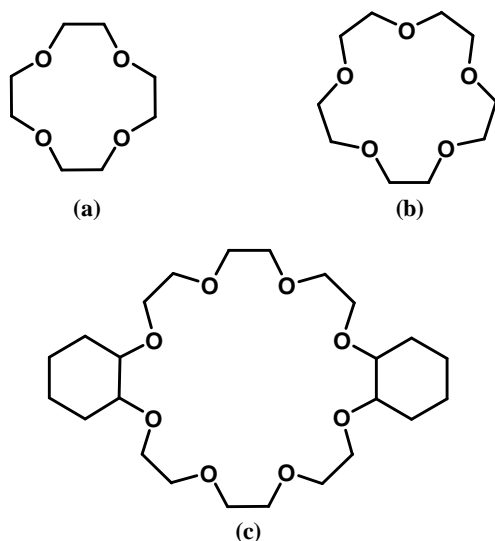


Figure 3 : Molecular structures of crown-ethers used in the PIMs: a) 12C4, b) 15C5, c) D24C8

## Analysis

The metal concentrations were determined by samplings at different time intervals aliquots of 1 ml each from the feed and strip solutions and analysed with flame atomic absorption spectrometry (AAS, Spectr AA-110, Varian). Mass flux  $J$  ( $\text{mol}\cdot\text{cm}^2\cdot\text{s}^{-1}$ ) of the metal ions through the PIM transferred from the feed side of the membrane to the strip side was determined applying its definition:  $J = \Delta n / S \Delta t$ , where  $\Delta n$  represents the variation in mole number of metal ions in the receiving solution during the reference time  $\Delta t$ , and  $S$  is the membrane active surface. IR spectra were recorded on with Perkin-Elmer (Spectrum One) spectrophotometer. X-ray analyses were recorded on a BRUKER D8 diffractometer using monochromatic  $\text{CuK}\alpha$  radiation.

Scanning electron microscope (SEM) images of the PIMs were obtained using a JOEL JSM 6360-LV microscope after gold coating, operating at 10 kV.

The thermo-gravimetric analyses were achieved using a SETARAM TG 96, thermal analysis instrument programmed from 30 to 600 °C at rate of 10 °C/min under the nitrogen atmosphere.

## Transport

The cell used for transport experiments consisted of two compartments, made of teflon with a maximum filling volume of 50 ml, separated by the PIM. The feed compartment contains the metal solution at a concentration of  $10^{-2}$  M of metal salt; the other compartment noted strip contains distilled water. Each compartment was provided with a mechanical stirrer at stirring speed 800 rpm which was previously determined as high enough to minimize the thickness of the boundary layer. The experiments began when starting the stirring motors in the two compartments of the cell. The exposed membrane area was 9.61 cm<sup>2</sup>. All the experiments were performed in a thermostat at 25 °C.

## RESULTS AND DISCUSSION

### Physical and chemical characteristics of synthesized membranes

In TABLE 1, some of the characteristics of the

## Full Paper

membrane made with the carriers have been listed (thickness, water content). We observed that inclusion of carriers into the polymer inclusion membranes induced a remarkable increase of its thickness (20 $\mu\text{m}$  to 32 $\mu\text{m}$ ). As the carrier molecules are hydrophobic, the location of carrier molecules at the surface of the modified

**TABLE 1 : Chemical and physical characteristics of PIMs.**

Membrane	Thickness ( $\mu\text{m}$ )	Water Content (%)
CTA + TEHP + 12C4	28	8,06
CTA + TEHP + 15C5	20	7.58
CTA + TEHP + D24C8	24	0,12
CTA + PMMA + TEHP + 12C4	26	8.65
CTA + PMMA + TEHP + 15C5	32	0,06
CTA + PMMA + TEHP + D24C8	30	0,50
CTA + P4VP + TEHP + 12C4	27	4,76
CTA + P4VP + TEHP + 15C5	29	7,30
CTA + P4VP + TEHP + D12C8	21	3.11

membranes should modify the contact angle which is a parameter indicative of the wetting character of a material.

### X-ray diffraction

Figures 4-6 show the X-ray curves for polymer + plasticizer + carrier membrane. Based on these figures, we can observe the following: All synthesized membranes present a single maximum located at approximately 20° found in all polymers and corresponds to the Van der Waals halo. Thus, this material presents basically amorphous characteristics (all systems do not give any diffraction). It can be due to the absence of crystallization within the membrane. On the other hand, this result should be attributed to the amorphous state of the structure which permits us to eliminate the mechanism of transfer of the ions by successive jumps between carrier complexing sites in a 3D assembled state.

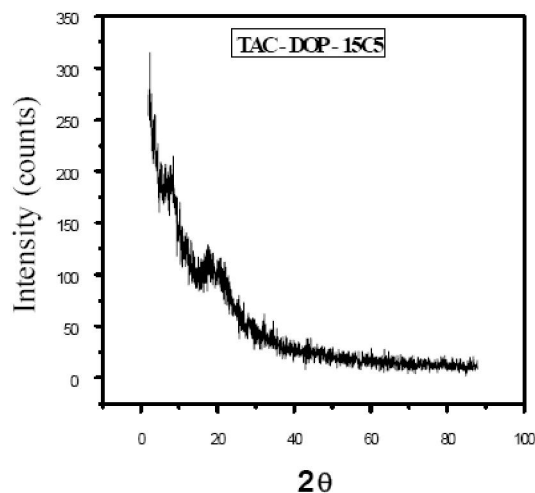
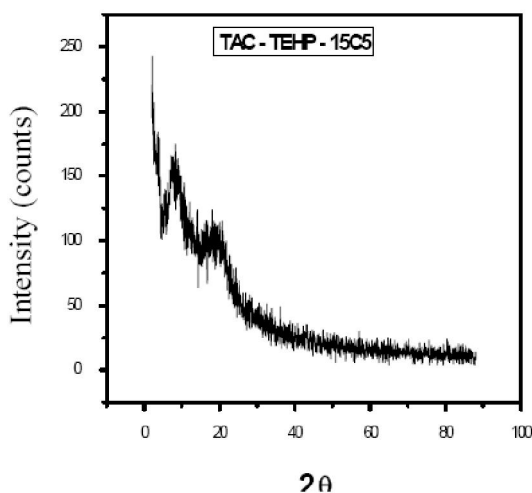


Figure 4 : X-ray diffractograms of membranes: (a) TAC-TEHP-15C5, (b) TAC-DOP-15C5

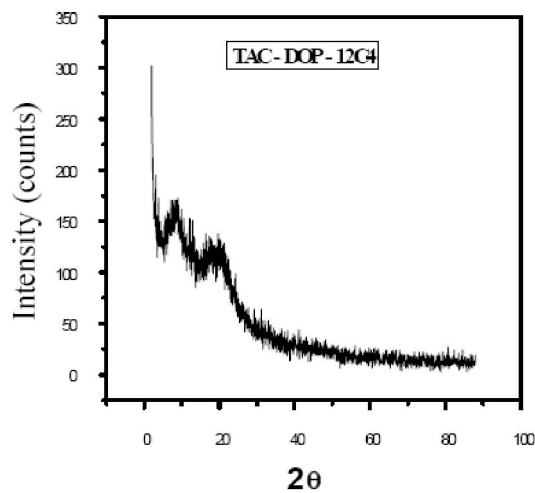
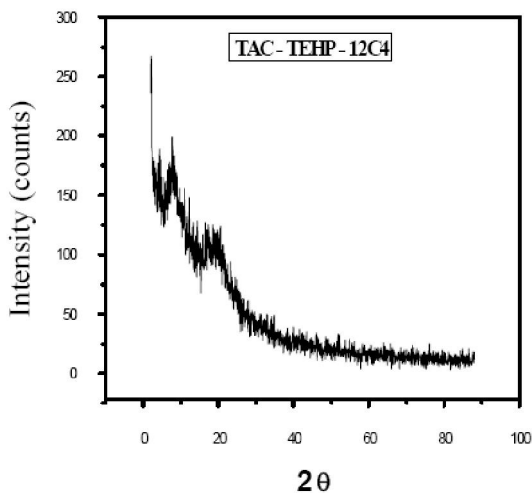


Figure 5 : X-ray diffractograms of membranes: (a) TAC-TEHP-12C4, (b) TAC-DOP-12C4

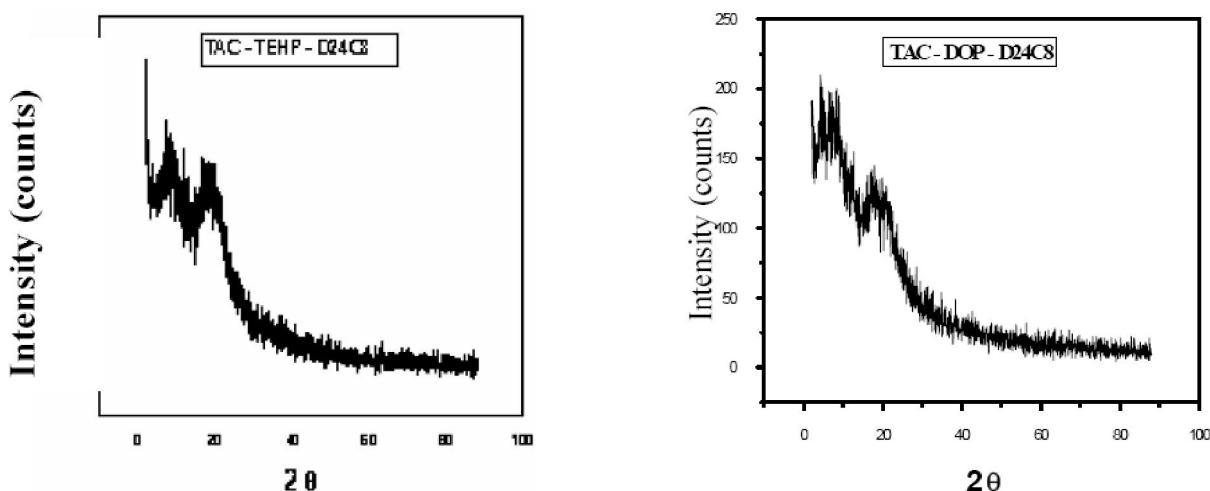


Figure 6 : X-ray diffractograms of membranes: (a) TAC-TEHP-D24C8, (b) TAC-DOP-D24C8

## FTIR

Figures 7-9 show respectively the spectrum of the cellulose triacetate + plasticizer + 12C4 membrane, cellulose triacetate + plasticizer + 15C5 membrane and cellulose triacetate + plasticizer + D24C8 membrane. The main feature of these spectrums is an absorption band located around  $1755\text{ cm}^{-1}$ , which is attributed to stretching vibrations of the carbonyl group. Bands at  $1237$  and  $1011\text{ cm}^{-1}$  correspond to the stretching modes of C–O bonds of carriers. Less intense bands at  $2922$  and  $2890\text{ cm}^{-1}$  are attributed to C–H bonds and the wide band detected in the  $3472$ – $3100\text{ cm}^{-1}$  region is attributed to the O–H bonds

stretching modes. The obtained results showed that all the maximum values extracted from the spectrum of the CTA reference membrane, i.e. without Plasticizer and carrier, are present in the modified membranes spectra in addition to those of the carrier molecules that also involve the same radicals.

TABLE 2 collects the peak values and the corresponding radical of polymer + plasticizer + carrier membranes. This should suggest that no signs of covalent bond formation between the carrier, plasticizer, and the base membrane skeleton, only weak interactions between constituents of the PIMs such as hydrophobic, Van der Waals and/or hydrogen bonds.

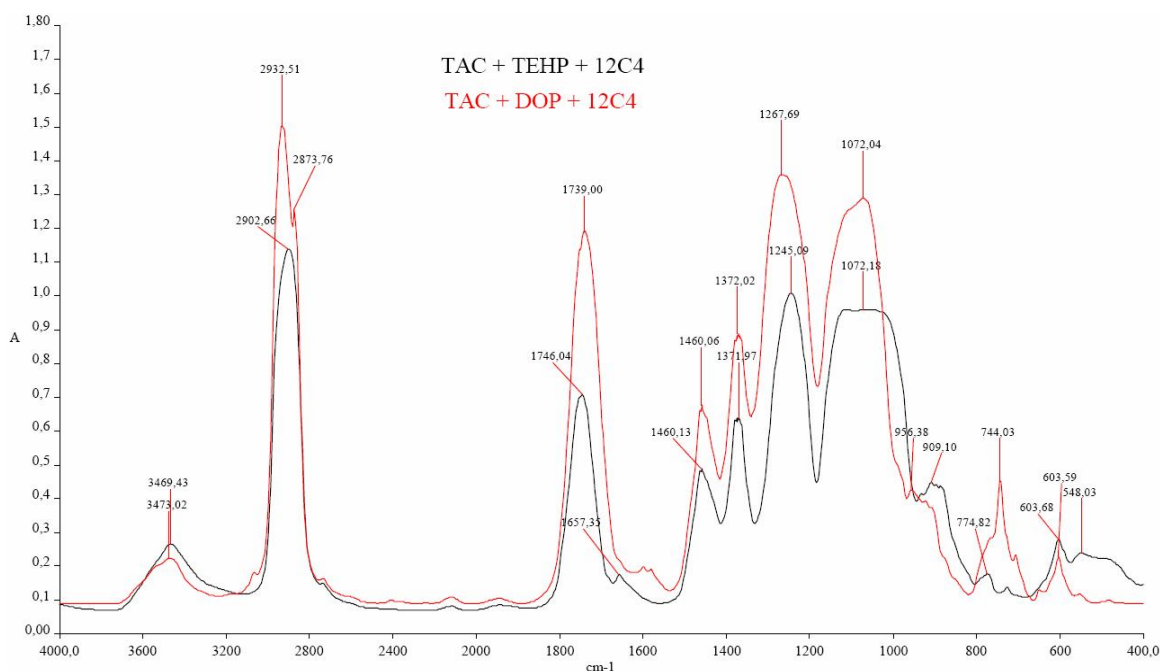


Figure 7 : FTIR spectrum of the (TAC + TEHP + 12C4) and (TAC + DOP + 12C4) membrane

## Full Paper

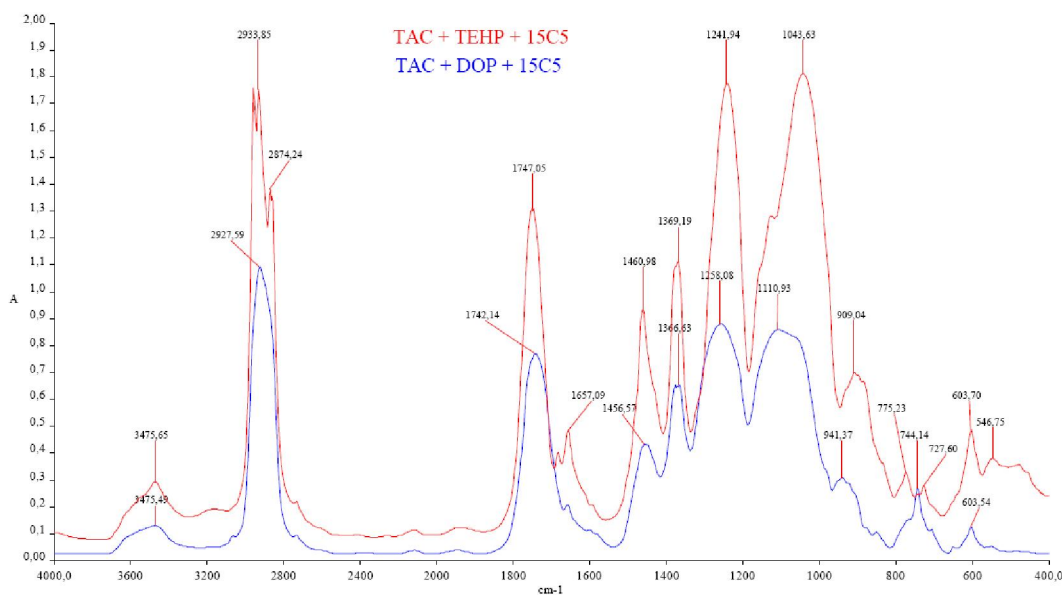


Figure 8 : FTIR spectrum (TAC + TEHP + 15C5) and (TAC + DOP + 15C5) membranes.

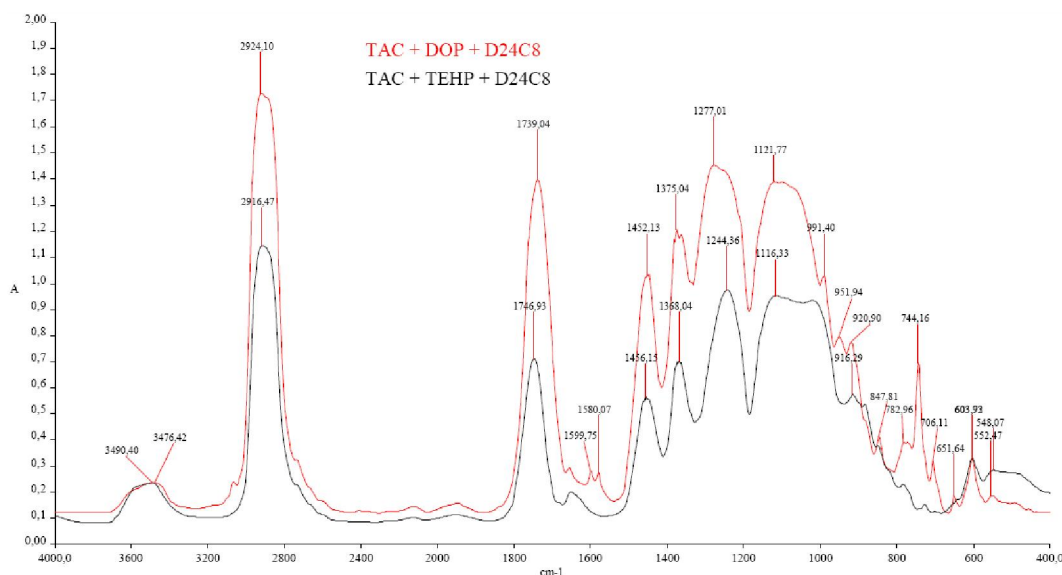


Figure 9 : FTIR spectrum of (TAC + TEHP + D24C8) and (TAC + DOP + D24C8) membranes

TABLE 2 : Peak values and the corresponding radical of the different membranes obtained by FTIR.

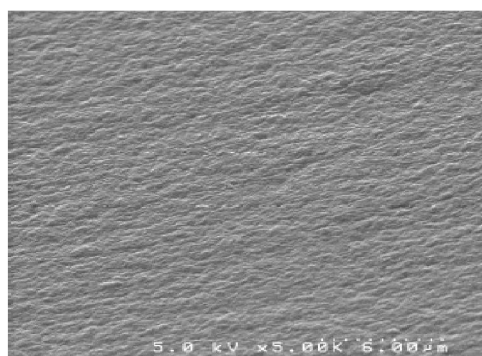
Membrane	Peak values (cm <sup>-1</sup> )	Corresponding Radical
CTA + Plasticizer + Crown-ethers	3469-3473	O – H
	2902-2932	C – H
	1731-1748	C = O
	1657	C = C (DOP)
	1460	– CH <sub>2</sub> (TAC)
	1372	– CH <sub>3</sub> (TAC)
	1245-1267	P=O (TEHP)
	1072	C – O – C (TAC)
	956	C – O – C (DOP)
	909	P – O – C (TEHP)

### Characterisation by scanning electron microscopy (SEM)

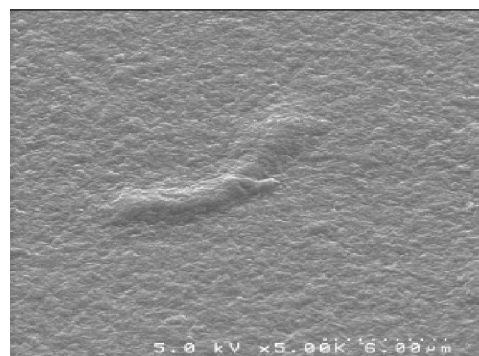
From SEM images (Figure 10), it can be observed that the morphologies of the polymer + plasticizer + carrier membranes had a uniform surface and appeared dense with no apparent porosity.

### Characterisation by thermo-gravimetric analysis (TGA)

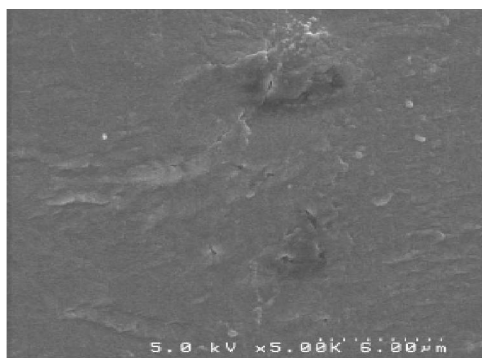
The TGA experiments were done using SETARAM TG 96 equipment. Figures 11-13 show respectively the TGA thermal behaviors of (CTA + TEHP + 15C5), (CTA + P4VP + TEHP + 15C5) and (CTA + PMMA



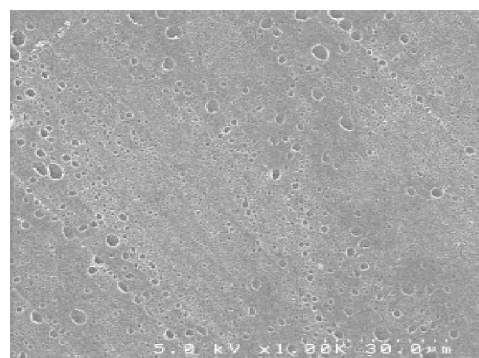
CTA+TEHP+15C5 (surface)



CTA+DOP+15C5 (surface)



CTA+P4VP+TEHP+15C5 (surface)



CTA+PMMA+DOP+15C5 (surface)

Figure 10 : Scanning electron microscopy of various membranes

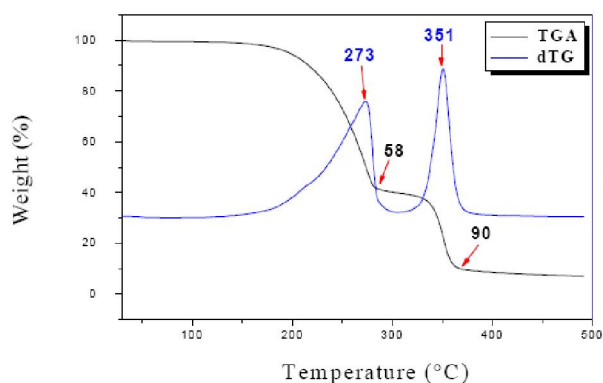


Figure 11 : Thermograms ATG/dTG of (CTA+TEHP+15C5) membrane.

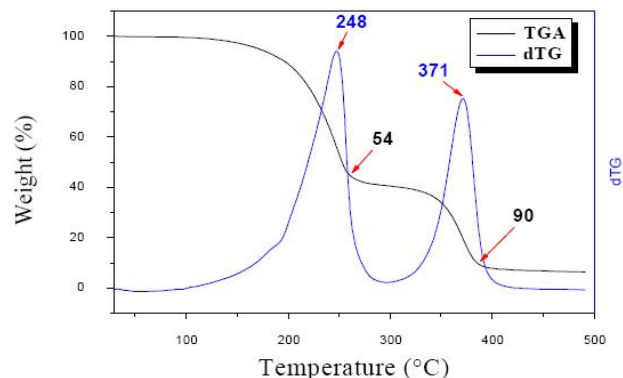


Figure 12 : Thermograms ATG/dTG of (CTA+P4VP+TEHP+15C5) membrane.

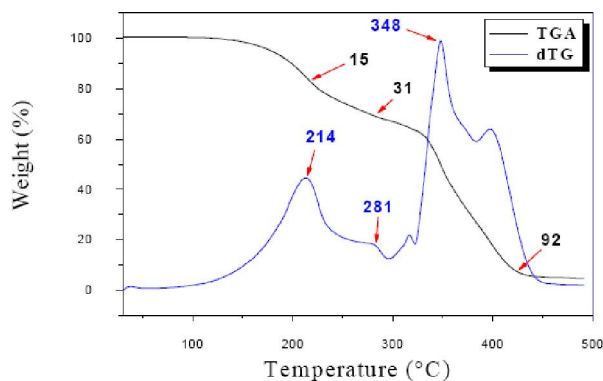


Figure 13 : Thermograms ATG/dTG of (CTA+PMMA+TEHP+15C5) membrane.

+ TEHP + 15C5) membranes. Based on these figures, the following observation can be made:

The synthesized membranes (CTA + TEHP + 15C5) and (CTA + P4VP + TEHP + 15C5) break in two steps. The first step at 200-250 °C represents the main thermal degradation of the polymeric chains. The second one starts at 350 °C and represents the carbonization of the products to ash.

The synthesized membrane (CTA + TEHP + PMMA + 15C5) degrades in three steps. The first one at 150-180°C represents the main thermal degradation of the PMMA chains. The second step at 200-250°C

## Full Paper

represents a degradation of CTA chains. The third step represents the carbonization of a degraded material.

### Influence of the carrier nature

The transport has been achieved with three macrocyclic polyethers, 12C4, 15C5 and D24C8.

Figures 14 and 15 represent the variation of copper (II) and zinc (II) quantities transferred versus the carrier nature using respectively TEHP and DOP as plasticizers. The results obtained show that 15C5 is the best carrier for two metallic ions. The selectivity at the interface is much higher when the metal cation is more inserted in the crown-ether cavity according to the ratio between the polyether cavity and the size of the inserted cation; copper (II) ions are more adaptable to the cavity of 15C5 than 12C4 and D24C8. This is due to the copper (II) ion size ( $1.38 \text{ \AA}$ ) which is nearest of the size of the cavity of 15C5 ( $1.50 \text{ \AA}$ ) compared to 12C4 ( $1.20 \text{ \AA}$ ) and D24C8 ( $2.6 \text{ \AA}$ ).

### Influence of the plasticizer nature

Plasticizers are well known compounds used in polymer processing to ensure flexibility and to avoid brittleness and cracking. In this study, two plasticizers (TEHP or DOP) were tested in the order to verify their effect on the copper (II) and zinc (II) transport through PIMs.

Figures 16a and 16b show respectively Cu(II) and Zn(II) concentrations in a strip phase using TEHP or DOP as plasticizers. It can be perceived that TEHP

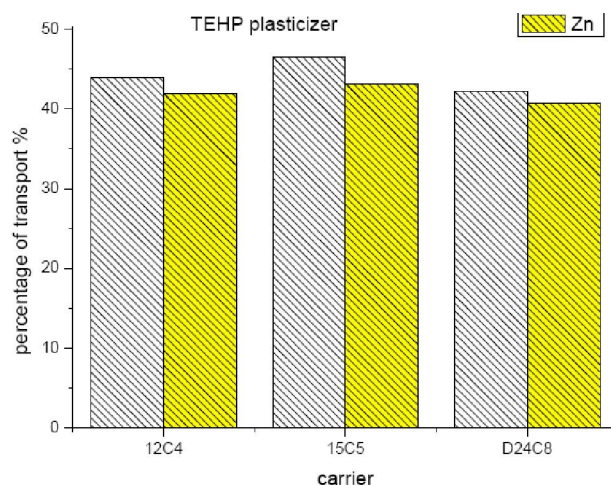


Figure 14 : Evolution of the concentration of metallic ions in the strip phase versus the carrier nature. Plasticizer: TEHP.

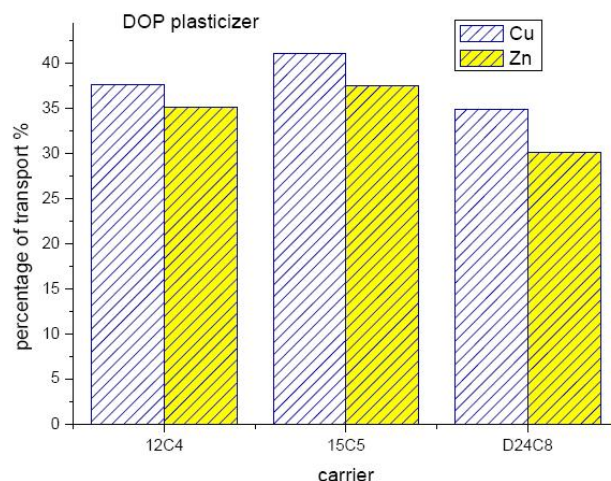


Figure 15 : Evolution of the concentration of metallic ions in the strip phase versus the carrier nature. Plasticizer: DOP.

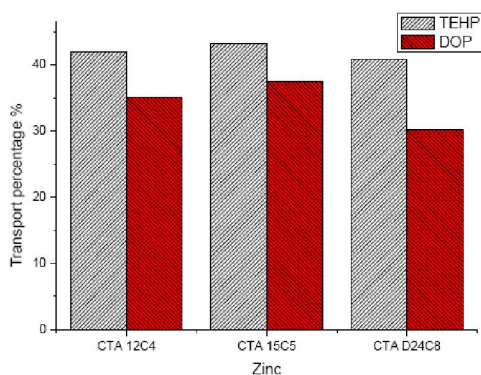


Figure 16 : Evolution of the concentration of metallic ions in the strip phase versus the plasticizer nature.

( $\eta = 10.2 \text{ cP}$ ,  $\epsilon_r = 4.8$ ) and DOP ( $\eta = 76 \text{ cP}$ ,  $\epsilon_r < 10$ ) produce the highest PIM transport of ions. Indeed, the plasticizer polarity influences the chemical potential of metal ion partitioning into the membrane, whereas increasing the viscosity of the plasticizer decreases the rate of transport, most likely by inhibiting

the diffusion process.

## CONCLUSION

A mixture of cellulose triacetate and poly-4-vinyl pyridine (P4VP) or polymethyl methacrylate (PMMA)

membrane containing crown-ethers as a carrier and triethylhexyl phosphate (TEHP) or Dioctyl phthalate (DOP) as plasticizers have been synthesized. These Polymers + plasticizer + carrier membranes were characterized using chemical techniques as well as Fourier Transform Infrared (FTIR), X-Ray Diffraction (XRD), Thermogravimetric analysis (TGA) and Scanning Electron Microscopy (SEM). The systems constituted by the mixture of Polymer + Plasticizer + Carrier do not give any diffraction peak. It can be due to the absence of crystallization within the membrane. The synthesized membranes degrade in two steps. The first step at 200-250 °C represents the main thermal degradation of the polymeric chains. This result confirms that all synthesized membranes show a very good thermal stability. The synthesized membranes present a dense and homogeneous structure.

A comparative study of the transport across a polymer inclusion membrane (PIM) has shown that the copper (II) and zinc (II) transport efficiency was increased using a modified PIM.

This approach opens large perspectives for utilizing the crown-ethers carrier mediated transport technique in the treatment of hydrometallurgical solutions. Further efforts will be directed to the determination of the nature of interactions between polymer and carrier by use of other materials and analysis as well.

## REFERENCES

- [1] J.D.Lamb, R.L.Bruening, R.M.Izatt, Y.Hirashima, P.Tse, J.J.Christensen; *J.Membr.Sci.*, **37**, 13-26 (1988).
- [2] W.F.Nejenhuis, A.R.Van Doom, A.M.Reichwein, F.De Jong, D.N.Reinhoudt; *J.Am.Chem.Soc.*, **113**, 3607-3608 (1991).
- [3] T.M.Fyles, C.A.Mac Gavin, D.E.Thompson; *J.Chem.Soc., Chem.Comm.*, 924-938 (1982).
- [4] W.Walkowiak, C.A.Kozlowski; *Desalination*, **240**, 186-197 (2009).
- [5] A.A.Amiri, A.Safavi, A.R.Hasaninejad, H.Shrghi, M.Shamsipur; *J.Membr.Sci.*, **325**, 295-300 (2008).
- [6] J.de Gyves, Rodriguez E.de San Miguel; *Ind.Eng.Chem.Res.*, **38**, 2182 (1999).
- [7] J.Marchese, F.Valenzuela, C.Basualto, A.Acosta; *Hydrometallurgy*, **72**, 309-317 (2004).
- [8] K.Sarangi, R.P.Das; *Hydrometallurgy*, **71**, 335-342 (2004).
- [9] A.Gherrou, H.Kerdjoudj, R.Molinari, E.Drioli; *Sep.Sci.Technol.*, **37**, 2317-2336 (2002).
- [10] A.Gherrou, H.Kerdjoudj, R.Molinari, E.Drioli; *J.Memb.Sci.*, **272**, 143-151 (2006).
- [11] A.Gherrou, H.Kerdjoudj; *Desalination*, **144**, 231-236 (2002).
- [12] A.Gherrou, H.Kerdjoudj, R.Molinari, E.Drioli; *Sep.Purif.Technol.*, **22**, 571-581 (2001).
- [13] J.M.Joshi, P.N.Pathak, A.K.Pandey, V.K.Man-chanda; *Hydrometallurgy*, **96**, 117-122 (2009).
- [14] O.Arous, A.Gherrou, H.Kerdjoudj; *Desalination*, **161**, 295-303 (2004).
- [15] O.Arous, A.Gherrou, H.Kerdjoudj; *Sep.Sci.Technol.*, **39**, 1681-1693 (2004).
- [16] P.K.Mohapatra, D.S.Lakshmi, D.Mohan, V.K.Man-chanda; *J.Membr.Sci.*, **232**, 133-139 (2004).
- [17] S.Sriram, P.K.Mohapatra, A.K.Pandey, V.K.Man-chanda, L.P.Badheka; *J.Membr.Sci.*, **177**, 163 (2000).
- [18] P.R.Danesi; *Sep.Sci.and Tech.*, **19**, 857 (1985).
- [19] P.K.Mohapatra, D.S.Lakshmi, D.Mohan, V.K.Man-chanda; *J.Membr.Sci.*, **232**, 133 (2004).
- [20] M.Sugiura; *Sep.Sci.Technol.*, **28**, 1456 (1993).
- [21] O.Arous, H.Kerdjoudj, P.Seta; *J.Membr.Sci.*, **241**, 177 (2004).
- [22] L.D.Nghiem, P.Mornane, I.D.Potter, J.M.Perera, R.W.Cattrall, S.D.Kolev; *J.Membr.Sci.*, **281**, 7 (2006).
- [23] N.Pereira, A.St John, R.W.Cattrall, J.M.Perer, S.D.Kolev; *Desalination*, **236**, 327 (2009).
- [24] M.Ulewicz, U.Lesinska, M.Bochenska; *Physico-chem.Probl.Miner.Process*, **44**, 245-256 (2010).
- [25] S.A.Ansari, P.K.Mohapatra, D.R.Raut, M.Kumar, B.Rajeswari, V.K.Man-chanda; *J.Membr.Sci.*, **337**, 304 (2009).
- [26] G.Levin, L.Bromberg; *J.Appl.Polym.Sci.*, **48**, 335 (1993).
- [27] G.Argiropoulos, R.W.Cattrall, I.C.Hamilton, S.D.Kolev, R.Paimin; *J.Membr.Sci.*, **138**, 279 (1998).
- [28] M.F.Paugam, J.Buffle; *J.Membr.Sci.*, **147**, 207-215 (1998).
- [29] A.J.Schow, R.T.Peterson, J.D.Lamb; *J.Membr.Sci.*, **111**, 291-295 (1996).
- [30] M.Sugiura, M.Kikkawa, S.Urita; *J.Membr.Sci.*, **42**, 47 (1989).